

# Selective chemical vapor deposition of HfB<sub>2</sub> on Al<sub>2</sub>O<sub>3</sub> over SiO<sub>2</sub> and the acceleration of nucleation on SiO<sub>2</sub> by pretreatment with Hf[N(CH<sub>3</sub>)<sub>2</sub>]<sub>4</sub>

---

Cite as: J. Vac. Sci. Technol. A **39**, 023415 (2021); <https://doi.org/10.1116/6.0000691>

Submitted: 04 October 2020 . Accepted: 04 February 2021 . Published Online: 02 March 2021

---

Zhejun V. Zhang, Sumeng Liu, Gregory S. Girolami, and John R. Abelson

---

## COLLECTIONS

Paper published as part of the special topic on [Special Topic Collection on Area Selective Deposition](#)

 This paper was selected as Featured



[View Online](#)



[Export Citation](#)



[CrossMark](#)

---

## ARTICLES YOU MAY BE INTERESTED IN

[Ultrasmooth cobalt films on SiO<sub>2</sub> by chemical vapor deposition using a nucleation promoter and a growth inhibitor](#)

Journal of Vacuum Science & Technology A **39**, 023414 (2021); <https://doi.org/10.1116/6.0000688>

[Next generation nanopatterning using small molecule inhibitors for area-selective atomic layer deposition](#)

Journal of Vacuum Science & Technology A **39**, 021002 (2021); <https://doi.org/10.1116/6.0000840>

[Conversion reactions in atomic layer processing with emphasis on ZnO conversion to Al<sub>2</sub>O<sub>3</sub> by trimethylaluminum](#)

Journal of Vacuum Science & Technology A **39**, 021001 (2021); <https://doi.org/10.1116/6.0000680>



Advance your science and  
career as a member of

**AVS**

LEARN MORE >

# Selective chemical vapor deposition of HfB<sub>2</sub> on Al<sub>2</sub>O<sub>3</sub> over SiO<sub>2</sub> and the acceleration of nucleation on SiO<sub>2</sub> by pretreatment with Hf[N(CH<sub>3</sub>)<sub>2</sub>]<sub>4</sub>

Cite as: J. Vac. Sci. Technol. A 39, 023415 (2021); doi: 10.1116/6.0000691

Submitted: 4 October 2020 · Accepted: 4 February 2021 ·

Published Online: 2 March 2021



View Online



Export Citation



CrossMark

Zhejun V. Zhang,<sup>1</sup> Sumeng Liu,<sup>2</sup> Gregory S. Cirolami,<sup>2</sup> and John R. Abelson<sup>1,a)</sup>

## AFFILIATIONS

<sup>1</sup>Department of Materials Science and Engineering, University of Illinois at Urbana-Champaign, 1304 W. Green St., Urbana, Illinois 61801

<sup>2</sup>School of Chemical Sciences, University of Illinois at Urbana-Champaign, 600 South Mathews Avenue, Urbana, Illinois 61801

**Note:** This paper is a part of the Special Topic Collection on Area Selective Deposition.

<sup>a</sup>Electronic mail: [abelson@illinois.edu](mailto:abelson@illinois.edu)

## ABSTRACT

We show that growth of the metallic ceramic HfB<sub>2</sub> by CVD from Hf(BH<sub>4</sub>)<sub>4</sub> at 220 °C is inherently selective on Al<sub>2</sub>O<sub>3</sub> over SiO<sub>2</sub>: a 10.4-nm film grows on Al<sub>2</sub>O<sub>3</sub> in 16 min, whereas only 0.07 nm of HfB<sub>2</sub> grows on SiO<sub>2</sub> in 18 min. Nucleation occurs on both SiO<sub>2</sub> and Al<sub>2</sub>O<sub>3</sub>; however, the Al<sub>2</sub>O<sub>3</sub> surface has a much higher density of nuclei such that HfB<sub>2</sub> islands quickly coalesce to form continuous films, followed by steady-state growth of HfB<sub>2</sub>. On SiO<sub>2</sub>, nucleation is sparse and coalescence of the islands takes much longer; as a result, the overall growth rate is slower. Sparse nucleation on SiO<sub>2</sub> also leads to a rough layer with a broad height distribution function: for a deposit containing  $1.6 \times 10^{15}$  Hf atoms/cm<sup>2</sup> (equivalent to a bulk thickness of 0.5 nm for HfB<sub>2</sub>), the rms roughness is 3.8 nm on SiO<sub>2</sub> but only 1.3 nm on Al<sub>2</sub>O<sub>3</sub>. The difference in the formation rate of nuclei (and thus the area density of nuclei) is attributed to the different acid-base character of hydroxyl groups on these oxide surfaces. We also found that, when growth on SiO<sub>2</sub> is desired, the surface can be modified by exposure to tetrakis(dimethylamido)hafnium, which adsorbs to saturation at ~1 monolayer. Subsequent exposure of this pretreated surface leads to an increased density of HfB<sub>2</sub> nuclei, a reduced coalescence time, and a smaller roughness of the resulting surface from 3.8 to 1.7 nm. By contrast, a similar pretreatment on Al<sub>2</sub>O<sub>3</sub> has little effect on the roughness of subsequently grown HfB<sub>2</sub> films, which are already relatively smooth when grown on untreated alumina surfaces.

Published under license by AVS. <https://doi.org/10.1116/6.0000691>

## I. INTRODUCTION

Chemical vapor deposition (CVD) is a powerful technique for depositing very thin films.<sup>1,2</sup> One of the current challenges is developing CVD processes that deposit films on one surface but not another, called area-selective deposition (ASD). Such processes in principle guarantee pattern registry and as a result are likely to become increasingly important for the fabrication of future generations of integrated circuits. ASD occurs when the formation and growth of nuclei are kinetically rapid on one surface but very slow on another. An important goal is to understand the reasons why the nucleation process differs on different surfaces.

The most elementary kinetic description of nucleation includes three parameters: the area density of possible nucleation sites, the rate at which nuclei form on these sites, and the rate of

film growth on those nuclei. Additional factors, such as island shape and surface diffusion,<sup>2–4</sup> can also affect the nucleation process. To achieve ASD, the quantity of film deposited on the intended non-growth surface should be acceptably small—where the allowable limit is set by the device and fabrication process in question—during the time required to nucleate and grow the required thickness of film on the intended growth surface.<sup>5</sup> A challenge is to assure a sufficiently small density of nuclei on the nongrowth surface and, if possible, a small growth rate of those nuclei.

In addition, to achieve very smooth films on the intended growth surface, the precursor should have a high probability of reaction with the surface (a high nucleation rate) relative to the probability of reacting with the nuclei (a low growth rate). Under these conditions, a high areal density of small nuclei forms on the

substrate and then growth of these nuclei—possibly accompanied by continuous formation of additional nuclei—affords complete coalescence at a small thickness with low surface roughness.<sup>3,4,6,7</sup>

We have previously described techniques to modify the rate of nucleation of Co films from the precursor  $\text{Co}_2(\text{CO})_8$ . That work showed how to achieve two opposite goals: (i) to suppress nucleation so that film nucleation and growth occur only on some substrate materials and not on others;<sup>9</sup> and (ii) to enhance nucleation so that the resulting films are ultrasmooth.<sup>8</sup>

Here, we consider the same goals for the nucleation of  $\text{HfB}_2$  on oxides by CVD from the precursor  $\text{Hf}(\text{BH}_4)_4$ .<sup>10</sup>  $\text{HfB}_2$  is a metallic ceramic material with good electrical conductivity, high hardness, low friction and wear, and excellent diffusion barrier properties.<sup>11</sup> At temperatures below 300 °C, film growth from this precursor is highly conformal in deep trenches and can coat and infill porous materials.<sup>12</sup> We previously described a method to enhance the nucleation density of  $\text{HfB}_2$  on c-Si, based on remote plasma treatment of the substrate surface,<sup>13</sup> and a method to limit the growth rate of  $\text{HfB}_2$  islands on  $\text{SiO}_2$ , based on coflow of a molecular inhibitor.<sup>14</sup>

The present work introduces two new effects: first, we show that deposition of  $\text{HfB}_2$  can be achieved selectively *on acidic oxides substrates but not on basic oxides*, e.g., nucleation and growth on  $\text{Al}_2\text{O}_3$  is fast but on  $\text{SiO}_2$  is slow; and second, pretreatment of an  $\text{SiO}_2$  surface with tetrakis(dimethylamido)hafnium (TDMAH) greatly enhances nucleation on this surface, and thus enables the growth of ultrasmooth films.

## II. EXPERIMENT

CVD experiments are performed in a cold wall turbopumped growth chamber of high vacuum construction described elsewhere; the base pressure is  $5 \times 10^{-8}$  Torr, most of which is  $\text{H}_2$ .<sup>10,15</sup> The precursor  $\text{Hf}(\text{BH}_4)_4$  is synthesized from  $\text{LiBH}_4$  and  $\text{HfCl}_4$  by a literature route originally developed for the zirconium analog.<sup>16</sup> The precursor is maintained in a stainless steel container immersed in a water bath and delivered to the chamber without a carrier gas through a 0.4 cm i.d. stainless steel tube aimed at the substrate to sustain a chamber pressure of 0.05 mTorr. The forward-directed gas stream produces a flux at the substrate surface that is approximately a factor of 2 higher than indicated by the isotropic background chamber pressure, which is measured by a capacitance manometer. TDMAH is supplied by Sigma-Aldrich and used as received. It is maintained in a separate metal container and is supplied at room temperature without carrier gas through a separate stainless steel tube aimed at the substrate. The pressure of precursors in the chamber is below the detection limit of the manometer ( $\sim 10^{-6}$  Torr). Substrates are radiatively heated to 220 °C, as measured by a K-type thermocouple attached to the front of the sample holder. For the samples with the pretreatment step, the  $\text{SiO}_2$  surface is exposed to TDMAH for 2 min at a temperature of 220 °C. In another study (manuscript in preparation), we investigate a dosing time of 30 s to 10 min on CVD of cobalt (manuscript in review). The adsorption saturates fast on the oxide (<30 s). When the dosing time is larger than 30 s, we did not observe any difference on film roughness and nucleation rate.  $\text{HfB}_2$  deposition is performed 8 min after the pretreatment, so that residual

TDMAH molecules that desorb from the room temperature chamber walls are pumped away.

Substrates are microelectronic grade Si wafers with 300 nm thermal  $\text{SiO}_2$  or 10 nm  $\text{Al}_2\text{O}_3$  deposited by atomic layer deposition (ALD) from trimethylaluminum and water at 80 °C. They are degreased by washing successively with acetone, isopropyl alcohol (IPA), and de-ionized water, and then cleaned by UV ozone treatment for 10 min before the substrates are loaded into the chamber. From our previous work,<sup>9</sup> this cleaning process affords a reliable starting surface for deposition.

To detect and quantify areal densities of nuclei, we use two tools: *in situ* ellipsometry and *ex situ* atomic force microscopy (AFM). Spectroscopic ellipsometry (SE) has proved to exhibit reproducible changes when nuclei form on the surface with sufficient size and density.<sup>17</sup> Because the initial morphology is highly anisotropic, it is not physically meaningful to fit data using simple assumptions in an effective medium theory, and thus, we report change in the ellipsometric angle  $\Psi$  at a single energy, 2.65 eV, which provides the greatest sensitivity to the onset of nucleation, as discussed previously. However, AFM is able to detect a very low density of islands, even on surfaces for which ellipsometry detects nothing. Nuclei densities are obtained by counting islands in  $500 \times 500$  nm AFM images of  $\text{SiO}_2$  substrates and in  $250 \times 250$  nm images of  $\text{Al}_2\text{O}_3$  substrates. The counting was carried out in quadruplicate for each sample to calculate a standard deviation. Note that tip convolution effects set a limit on the ability to resolve islands as separate when they are very close to each other. Film roughness is also measured by AFM.

The areal density of metal atoms is measured *ex situ* by Rutherford backscattering spectroscopy (RBS); we report an equivalent film thickness by fitting the areal atomic density of Hf atoms and converting it to film thickness using the bulk density of Hf atoms in stoichiometric  $\text{HfB}_2$ . Unless stated otherwise, all thicknesses are equivalent film thicknesses; in a previous work, we found that the density of  $\text{HfB}_2$  grown in this temperature range is  $\sim 30\%$  less than bulk.<sup>12</sup> For samples that have been pretreated with TDMAH, the resulting density of Hf atoms on the surface<sup>8</sup> is  $\sim 4.6 \times 10^{14} / \text{cm}^2$ ; this number is subtracted from the areal density of Hf atoms after exposure to  $\text{Hf}(\text{BH}_4)_4$  to obtain the amount of film deposited from the latter molecule.

The growth of thick films, i.e., beyond the nucleation and coalescence stage, is measured by SE. Data versus time are fit using a Lorentz oscillator model<sup>18</sup> for the optical properties of bulk  $\text{HfB}_2$ , and a multilayer optical model (in the COMPLETEEASE® software) to extract the film thickness. The model includes an effective medium representation of surface roughness; the thickness of the roughness layer varies from 1 to 5 nm in order to minimize the mean squared error of the fit.

## III. RESULTS AND DISCUSSION

### A. ASD of $\text{HfB}_2$ on $\text{SiO}_2$ and $\text{Al}_2\text{O}_3$

When  $\text{Al}_2\text{O}_3$  substrates are exposed to  $\text{Hf}(\text{BH}_4)_4$  for various times at 220 °C, SE detects the onset of  $\text{HfB}_2$  deposition in <2 min (Fig. 1), i.e., the nucleation delay is relatively short. The deposition rate increases with time and, following coalescence of the nuclei into a continuous film at  $\sim 5$  min, stabilizes at  $\sim 1.5 \text{ nm/min}$  (from

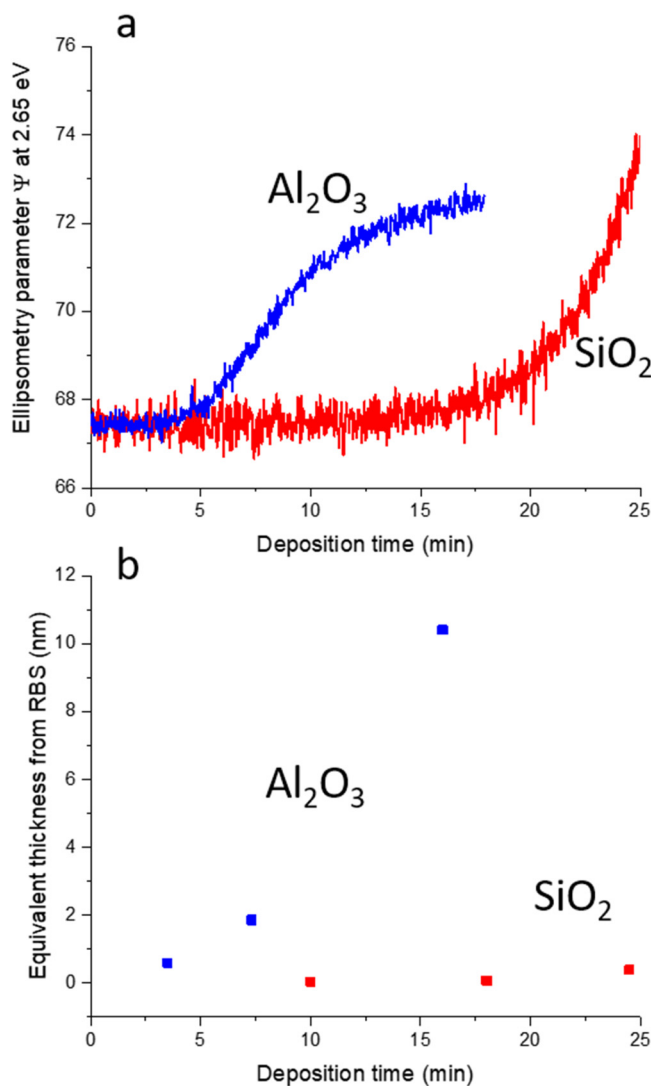


FIG. 1. (a) *In situ* ellipsometry parameter  $\Psi$ , at a photon energy of 2.65 eV, vs time for  $\text{HfB}_2$  deposition from  $\text{Hf}(\text{BH}_4)_4$  on  $\text{SiO}_2$  and  $\text{Al}_2\text{O}_3$ . (b)  $\text{HfB}_2$  equivalent film thickness measured by RBS vs deposition time. The RBS fit assumes bulk film density.

SE) or  $\sim 1 \text{ nm/min}$  (from RBS). (The disagreement between RBS and SE measurements of thickness is expected due to the reduced physical density and the surface roughness of the films; RBS is quantitative in terms of Hf coverage per area.) A 10.4 nm film (from RBS) is grown on  $\text{Al}_2\text{O}_3$  in 16 min.

The conclusion that nucleation is fast on  $\text{Al}_2\text{O}_3$  is confirmed by AFM images, which show that there are  $\sim 4300$  nuclei per  $\mu\text{m}^2$  after 3.5 min of exposure to  $\text{Hf}(\text{BH}_4)_4$  (Table I). The surface quickly reaches coalescence, after which the maximum height—which then represents the peak to valley roughness—is relatively constant.

In contrast, when  $\text{SiO}_2$  substrates are exposed to  $\text{Hf}(\text{BH}_4)_4$  for various times at  $220^\circ\text{C}$ , the nucleation delay (from SE) is more than 15 min and only 0.07 nm of  $\text{HfB}_2$  (by RBS) is deposited in 18 min. Thus, deposition of  $\text{HfB}_2$  is inherently selective on  $\text{Al}_2\text{O}_3$  over  $\text{SiO}_2$ , as shown by the ratio of deposited material of  $\sim 150:1$  for these conditions.

Although SE detects no nucleation on  $\text{SiO}_2$  over the first 15 min, some islands are formed on the surface during this time as shown by RBS and AFM: for a deposition time of 10 min, the RBS equivalent thickness is 0.015 nm, and AFM reveals the presence of  $110 \pm 35$  nuclei per  $\mu\text{m}^2$  having a maximum height of  $\sim 8$  nm (Fig. 2 and Table I). The AFM-determined density of nuclei increases linearly with deposition time (Table I and Fig. S2 in the supplementary material<sup>19</sup>), and extrapolation back to zero density suggests that nucleation begins at  $\sim 6$  min. Because islands with height  $\leq 2$  nm are generally not detectable by AFM because they are comparable to fluctuations in the substrate height, nucleation probably commences in less than 6 min.

At any one time, the number of islands decreases monotonically with height [Figs. S3(c) and S3(d) in the supplementary material<sup>19</sup>], a dependence that corresponds to continuous formation of nuclei over time.<sup>20</sup> If, instead, nucleation had occurred in a narrow time interval (e.g., near  $t = 0$ ), then the height distribution would exhibit a peak that shifts to greater heights as deposition proceeds. The maximum height increases linearly with growth time, with an intercept close to  $t = 0$  (Fig. 3); this time dependence<sup>21</sup> indicates that nucleation commences almost immediately upon exposure of the  $\text{SiO}_2$  surface to the  $\text{Hf}(\text{BH}_4)_4$  precursor. There is also a linear correlation between island radius, and height [Figs. S3(a) and S3(b) in the supplementary material<sup>19</sup>], consistent with conservation of island shape. Of course, the maximum height in AFM represents an island height only when the lowest point(s) in the image correspond to the bare substrate, i.e., before coalescence. That is the case for these data.

These results show that, between  $t = 0$  and coalescence, the net  $\text{HfB}_2$  growth rate (accumulation of material) is much faster on  $\text{Al}_2\text{O}_3$  than on  $\text{SiO}_2$  due to the higher nucleation rate and the higher density of nuclei on the former surface. For example, on  $\text{Al}_2\text{O}_3$ , it takes only 3.5 min to reach an equivalent thickness of 0.59 nm, whereas on  $\text{SiO}_2$ , it takes 24.5 min to reach an equivalent thickness of 0.39 nm. A possible means to further enhance the selectivity for growth on  $\text{Al}_2\text{O}_3$  would be to perform a periodic etch, which would remove the small number of stray nuclei on  $\text{SiO}_2$ ; such a protocol would also remove tall islands on the  $\text{Al}_2\text{O}_3$  surface (e.g., 8 nm), which are undesirable for many applications.<sup>22–24</sup>

In addition to the faster nucleation on  $\text{Al}_2\text{O}_3$ , the growth rate of individual islands is faster on  $\text{Al}_2\text{O}_3$  than on  $\text{SiO}_2$ ; on  $\text{Al}_2\text{O}_3$ , the tallest islands reach  $\sim 8$  nm in only in 3.5 min, whereas on  $\text{SiO}_2$ , the tallest islands reach  $\sim 8$  nm after 10 min of deposition. The mechanism responsible for this difference is unknown, but it may involve the rate at which adspecies—either precursor or by-product—can be transported between the island surface and the bare substrate by diffusion.

There is a temperature “window” for successful ASD; for that reason, the present work utilizes a fixed temperature of  $220^\circ\text{C}$ . At higher temperatures (such as  $250^\circ\text{C}$ ), deposition of  $\text{HfB}_2$  is fast on

**TABLE I.** Deposition of HfB<sub>2</sub> at 220 °C on SiO<sub>2</sub> and Al<sub>2</sub>O<sub>3</sub>, in some cases after pretreatment with TDMAH.

Substrate	Deposition time (min)	Equivalent thickness (nm)	rms roughness (nm)	Nuclei density ( $\mu\text{m}^{-2}$ )	Average nucleation rate ( $\mu\text{m}^{-2} \text{min}^{-1}$ )
Al <sub>2</sub> O <sub>3</sub>	3.5	0.59	1.3	$4300 \pm 360$	1230
SiO <sub>2</sub>	10	0.015	0.3 <sup>b</sup>	$110 \pm 30$	11
SiO <sub>2</sub>	18	0.07	1.7	$520 \pm 30$	29
SiO <sub>2</sub>	24.5	0.39	3.8	$730 \pm 60$	30
SiO <sub>2</sub>	34	5.8	4.6	$1000 \pm 60$	30
SiO <sub>2</sub> <sup>a</sup>	16.5	0.42	1.7	$2600 \pm 80$	156
Al <sub>2</sub> O <sub>3</sub>	7.3	1.9	1.4		Continuous films
Al <sub>2</sub> O <sub>3</sub>	16	10.4	1.1		Continuous films
Al <sub>2</sub> O <sub>3</sub> <sup>a</sup>	8.3	1.9	1.7		Continuous films

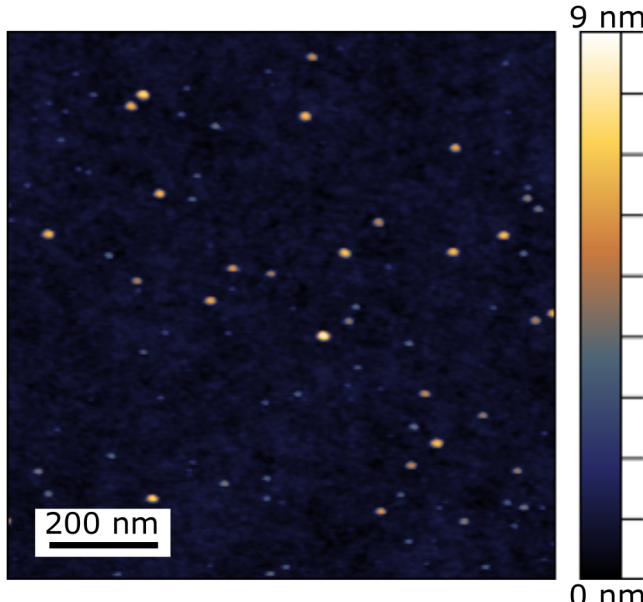
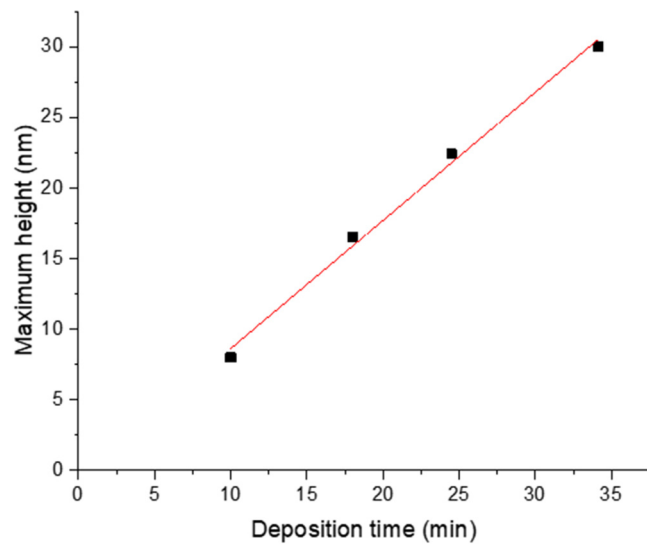
<sup>a</sup>With TDMAH pretreatment.<sup>b</sup>Before coalescence of nuclei, the roughness is dependent on the equivalent thickness (deposited atoms per area) and roughness is meaningful only when similar thicknesses are compared between samples. The rms roughness on the SiO<sub>2</sub> substrate with a 10-min growth time (second row in the table) is very low because most of the surface is bare; hence, the roughness is dominated by the very smooth SiO<sub>2</sub> surface.

both Al<sub>2</sub>O<sub>3</sub> and SiO<sub>2</sub>. At lower temperatures (such as 200 °C), deposition is very slow and the total growth time is unacceptably long [Fig. S1 in the supplementary material<sup>19</sup>]. Furthermore, at low temperature, a large fraction of the Hf(BH<sub>4</sub>)<sub>4</sub> precursor molecules are wasted (i.e., they pass through the chamber without reacting) during growth due to their lower reactivity.

### B. Film roughness on Al<sub>2</sub>O<sub>3</sub> and SiO<sub>2</sub>

In power spectral density (PSD) analysis, the amplitude at high spatial frequencies corresponds to short-range roughness on

the surface, and the amplitude at low frequencies corresponds to long-range roughness; the integral over the PSD distribution in a limited frequency range is related to the square of the rms roughness of the surface.<sup>25</sup> For the ~0.5 nm thick HfB<sub>2</sub> sample in Fig. 4, the PSD distribution exhibits a plateau at low  $k$  (i.e., distances longer than about 10 nm) that is an order of magnitude smaller on Al<sub>2</sub>O<sub>3</sub> than on SiO<sub>2</sub> (Fig. 5). This distribution indicates that the initially formed HfB<sub>2</sub> nuclei are significantly smoother on Al<sub>2</sub>O<sub>3</sub> than on SiO<sub>2</sub>, consistent with our previous work on film morphology as a function of nucleation density and island growth rate.<sup>8,14</sup> The similar magnitudes of the PSD at high  $k$  (i.e., distances shorter than 10 nm)

**FIG. 2.** AFM images of HfB<sub>2</sub> films on SiO<sub>2</sub> after 10 min of deposition at 220 °C.**FIG. 3.** Maximum height of HfB<sub>2</sub> islands on SiO<sub>2</sub> as a function of deposition time at 220 °C. The solid line is a least squares fit; the line has a slope of  $0.91 \text{ nm min}^{-1}$  and intercepts the x axis at 0.6 min. These data show that the island growth rate is constant, independent of the island size.

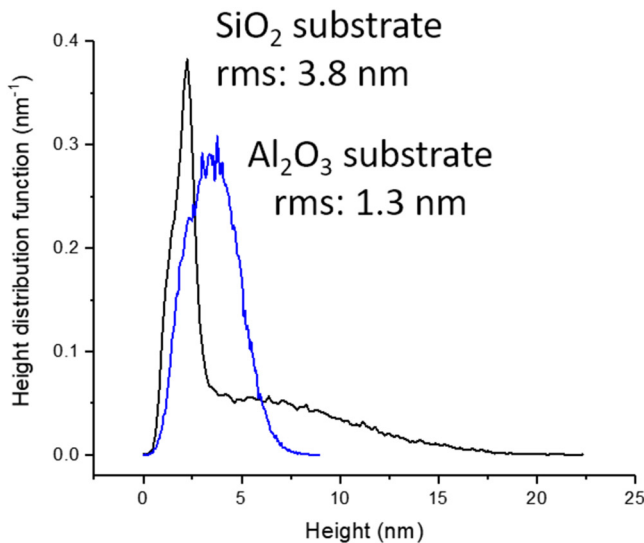
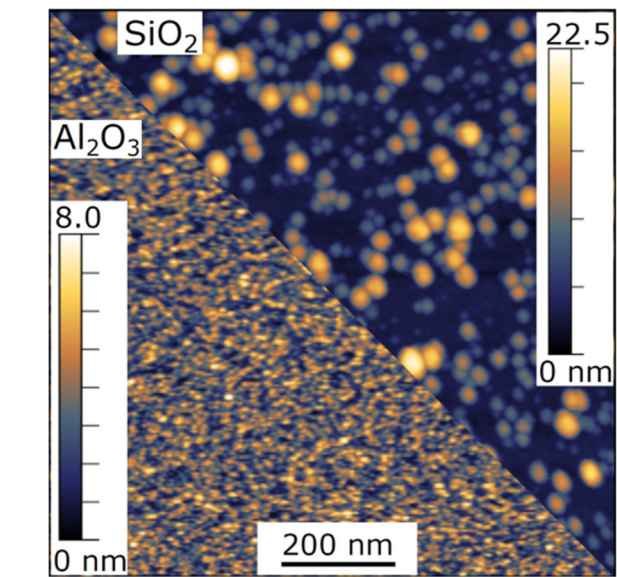


**FIG. 4.** AFM images and height distribution functions for  $\text{HfB}_2$  films of similar mean thicknesses (0.39 vs 0.59 nm) grown at 220 °C on  $\text{Al}_2\text{O}_3$  and  $\text{SiO}_2$  for deposition times of 3.5 and 24.5 min, respectively. On  $\text{Al}_2\text{O}_3$ , there is no substrate contribution to the data. On  $\text{SiO}_2$ , the sharp peak is mainly from the substrate surface and the broad shoulder is from the  $\text{HfB}_2$  islands.

indicate that short-range (local) smoothing mechanisms, such as diffusion of adspecies on the film surface, are likely active.

Oxide surface is typically covered by hydroxyl groups (OH) unless annealing in dry environment at high temperature.<sup>26</sup> And these hydroxyl groups have a basic or acidic character.<sup>27,28</sup> Nucleation of  $\text{HfB}_2$  likely takes place on these hydroxyl (—OH) groups. [In our previous work on Co growth, we indicated that siloxane rings are also good nucleation sites for  $\text{Co}_2(\text{CO})_8$ , but the density of these sites is significant only on highly dehydroxylated

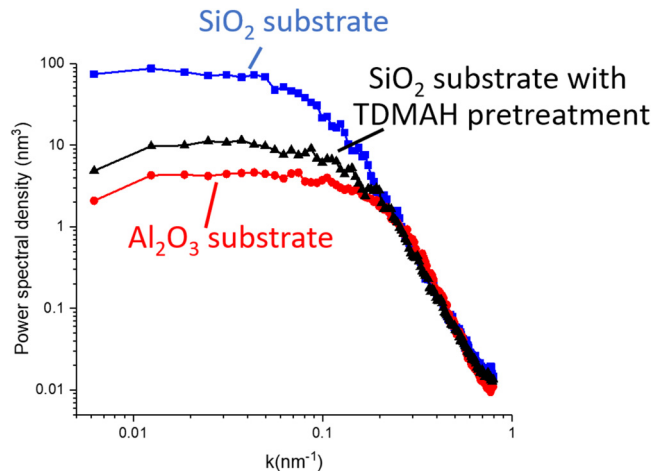


**FIG. 5.** Power spectral density of surface roughness from AFM data for the samples in **Fig. 4** and for an  $\text{SiO}_2$  substrate that had been pretreated with TDMAH. All samples have similar thicknesses (from top to bottom: 0.39, 0.42, and 0.59 nm). Deposition times are 24.5, 16.5, and 3.5 min.

$\text{SiO}_2$  surfaces.] On fully hydroxylated  $\text{Al}_2\text{O}_3$ , the density of OH groups<sup>29</sup> is  $\sim 10^7 \mu\text{m}^{-2}$  and on fully hydroxylated  $\text{SiO}_2$ , it is<sup>26</sup>  $\sim 4.6 \times 10^6 \mu\text{m}^{-2}$ . For the samples described above, the density of  $\text{HfB}_2$  nuclei is  $4300 \pm 362 \mu\text{m}^{-2}$  on  $\text{Al}_2\text{O}_3$  and  $730 \pm 65 \mu\text{m}^{-2}$  on  $\text{SiO}_2$ . Both densities are more than 3 orders of magnitude smaller than the respective hydroxyl densities; therefore, there is no depletion of available sites as nucleation occurs (Fig. S3 in the supplementary material<sup>19</sup>).

If we define the average nucleation rate as the density of nuclei divided by the growth time, then the rate (nucleation probability) on  $\text{Al}_2\text{O}_3$  is 40 times higher than on  $\text{SiO}_2$  (Table I). Although the cause of the higher nucleation probability on  $\text{Al}_2\text{O}_3$  is not known, we believe that the basicity of the oxide surface (hydroxyl groups) plays a significant role. First, Lewis bases are known to induce the decomposition of  $\text{Hf}(\text{BH}_4)_4$  to generate hafnium hydrides and borane-base adducts.<sup>30,31</sup> Because the  $\text{Al}_2\text{O}_3$  surface is more basic than  $\text{SiO}_2$ , similar decomposition reactions should be more favored on alumina than on silica. The net result would be that  $\text{Hf}(\text{BH}_4)_4$  precursor will transform to a nonvolatile reaction product; once the precursor can no longer desorb from the surface, it becomes a potential nucleation center. Second, when  $\text{M}(\text{BH}_4)_4$  ( $\text{M} = \text{Zr}$  and  $\text{Hf}$ ) molecules are adsorbed on alumina and silica, the surface-bonded  $\text{M}(\text{BH}_4)_x$  species decompose at lower temperature on  $\text{Al}_2\text{O}_3$  than on  $\text{SiO}_2$ .<sup>32</sup>

### C. Effect of TDMAH on $\text{HfB}_2$ nucleation

The above results show that  $\text{HfB}_2$  growth on  $\text{SiO}_2$  is slow to nucleate, which makes it difficult to grow a continuous thin film and the surface is very rough. We find that nucleation can be greatly accelerated on  $\text{SiO}_2$  by pretreatment of the surface with TDMAH. At 220 °C, adsorption of TDMAH is self-limiting, resulting in the formation of surface-bound  $\text{M}(\text{DMA})_x(\text{O}-\text{Si}=\text{O})_y$

intermediates.<sup>33–35</sup> HfB<sub>2</sub> growth on top of these intermediates is fast: a sample with an equivalent thickness of 0.42 nm is deposited in 16.5 min, which is 8 min shorter than the time required to grow a similarly thick film on a nontreated SiO<sub>2</sub> surface under otherwise identical conditions. Deposition of HfB<sub>2</sub> onto the pretreated sample affords a higher density of nuclei,  $\sim 2580 \pm 82 \mu\text{m}^{-2}$  (Table I and Fig. S4 in the supplementary material<sup>19</sup>), compared with  $733 \pm 65 \mu\text{m}^{-2}$  without pretreatment, leading to a much smaller roughness, 1.7 vs 3.8 nm. As judged from the PSD function, only long-range roughness is reduced whereas short-range roughness remains unchanged (Fig. 5). Thus, pretreatment of SiO<sub>2</sub> by exposure to TDMAH enhances nucleation and reduces the roughness of HfB<sub>2</sub> films grown by CVD from Hf(BH<sub>4</sub>)<sub>4</sub>. HfB<sub>2</sub> on the pretreated surface are, however, still not as smooth as on a native Al<sub>2</sub>O<sub>3</sub> surface.

In contrast to pretreatment of SiO<sub>2</sub>, TDMAH pretreatment of the Al<sub>2</sub>O<sub>3</sub> surface has little or no effect nucleation. It takes slightly longer (8.3 vs 7.3 min) to grow a film of similar thickness (1.9 nm) and the film is slightly rougher (1.7 vs 1.4 nm) (Table I and Fig. S5 in the supplementary material<sup>19</sup>).

One advantage of TDMAH is that it exhibits self-limiting adsorption when used as a precursor for ALD. This property means that nucleation enhancement by pretreatment of SiO<sub>2</sub> with TDMAH should also work in deep features.

#### IV. SUMMARY AND CONCLUSIONS

Selective deposition of HfB<sub>2</sub> on Al<sub>2</sub>O<sub>3</sub> over SiO<sub>2</sub> is demonstrated from the precursor Hf(BH<sub>4</sub>)<sub>4</sub> at 220 °C. Interestingly, nucleation occurs readily on both Al<sub>2</sub>O<sub>3</sub> and SiO<sub>2</sub>, but on Al<sub>2</sub>O<sub>3</sub>, the density of nuclei is a factor of 40 higher and the islands appear to grow twice as fast as on SiO<sub>2</sub>. The higher density leads to a smoother film on Al<sub>2</sub>O<sub>3</sub>: in the PSD, the low-frequency roughness is significantly lower for initially grown HfB<sub>2</sub> on Al<sub>2</sub>O<sub>3</sub> than SiO<sub>2</sub>. At an equivalent thickness of  $\sim 0.5$  nm, the rms roughness is  $\sim 1.3$  nm on Al<sub>2</sub>O<sub>3</sub> and  $\sim 3.8$  nm on SiO<sub>2</sub>. Pretreatment of SiO<sub>2</sub> surfaces by exposure to TDMAH increases the density of nuclei by a factor of 5 and reduces the rms roughness. However, TDMAH pretreatment of Al<sub>2</sub>O<sub>3</sub> surfaces does not improve (in fact, slightly degrades) the morphology of the films.

#### ACKNOWLEDGMENTS

We acknowledge the National Science Foundation for support of this work under Grant Nos. CMMI 1825938 (Z.V.Z. and J.R.A.) and CHE 1954745 (S.L. and G.S.G.). *Ex situ* materials characterization was carried out in the Center for Microanalysis of Materials at the Frederick Seitz Materials Research Laboratory, University of Illinois. We thank Kinsey L. Canova for help with preparation of figures.

#### DATA AVAILABILITY

The data that support the findings of this study are available within the article and its supplementary material.<sup>19</sup>

#### REFERENCES

- 1 A. E. Kaloyerous, Y. Pan, J. Goff, and B. Arkles, *ECS J. Solid State Sci. Technol.* **8**, P119 (2019).
- 2 J. Venables, *Introduction to Surface and Thin Film Processes* (Cambridge University, Cambridge, 2000).
- 3 P. Zhang, X. Zheng, S. Wu, and D. He, *Comput. Mater. Sci.* **30**, 331 (2004).
- 4 J. A. Venables and G. D. T. Spiller in *Surface Mobilities on Solid Materials: Fundamental Concepts and Applications*, edited by V. T. Binh (Springer US, Boston, MA, 1983), pp. 341–404.
- 5 W. L. Gladfelter, *Chem. Mater.* **5**, 1372 (1993).
- 6 S. Babar, “Role of growth inhibitors in nucleation and growth of thin film deposited by chemical vapor deposition in high aspect ratio structures, Doctoral dissertation,” Ph.D. thesis (University of Illinois at Urbana-Champaign, 2013).
- 7 H. A. Jehn, in *Advanced Techniques for Surface Engineering*, edited by W. Gissler and H. A. Jehn (Springer Netherlands, Dordrecht, 1992), pp. 5–29.
- 8 Z. V. Zhang, S. Liu, G. S. Girolami, and J. R. Abelson, “Ultrasmooth cobalt films on SiO<sub>2</sub> by chemical vapor deposition using a nucleation promoter and a growth inhibitor,” *J. Vac. Sci. Technol. A* (to be published).
- 9 Z. V. Zhang, S. Liu, G. S. Girolami, and J. R. Abelson, *J. Vac. Sci. Technol. A* **38**, 033401 (2020).
- 10 S. Jayaraman, Y. Yang, D. Y. Kim, G. S. Girolami, and J. R. Abelson, *J. Vac. Sci. Technol. A* **23**, 1619 (2005).
- 11 C. Mitterer, *J. Solid State Chem.* **133**, 279 (1997).
- 12 Y. Yang, S. Jayaraman, D. Y. Kim, G. S. Girolami, and J. R. Abelson, *Chem. Mater.* **18**, 5088 (2006).
- 13 N. Kumar, A. Yanguas-Gil, S. R. Daly, G. S. Girolami, and J. R. Abelson, *Appl. Phys. Lett.* **95**, 144107 (2009).
- 14 S. Babar, N. Kumar, P. Zhang, and J. R. Abelson, *Chem. Mater.* **25**, 662 (2013).
- 15 S. Jayaraman, E. J. Klein, Y. Yang, D. Y. Kim, G. S. Girolami, and J. R. Abelson, *J. Vac. Sci. Technol. A* **23**, 631 (2005).
- 16 W. E. Reid, J. M. Bish, and A. Brenner, *J. Electrochem. Soc.* **104**, 21 (1957).
- 17 S. Babar, E. Mohimi, B. Trinh, G. S. Girolami, and J. R. Abelson, *ECS J. Solid State Sci. Technol.* **4**, N60 (2015).
- 18 Y. Yang, S. Jayaraman, B. Sperling, D. Y. Kim, G. S. Girolami, and J. R. Abelson, *J. Vac. Sci. Technol. A* **25**, 200 (2007).
- 19 See supplementary material at <http://dx.doi.org/10.1116/6.0000691> for more ellipsometry and AFM data.
- 20 P. A. Mulheran and D. A. Robbie, *Europhys. Lett.* **49**, 617 (2000).
- 21 J. Soethoudt, F. Grillo, E. A. Marques, J. R. van Ommen, Y. Tomczak, L. Nyns, S. Van Elshocht, and A. Delabie, *Adv. Mater. Interfaces* **5**, 1800870 (2018).
- 22 M. F. J. Vos, S. N. Chopra, M. A. Verheijen, J. G. Ekerdt, S. Agarwal, W. M. M. Kessels, and A. J. M. Mackus, *Chem. Mater.* **31**, 3878 (2019).
- 23 S. K. Song, H. Saare, and G. N. Parsons, *Chem. Mater.* **31**, 4793 (2019).
- 24 W. Xie and G. N. Parsons, *J. Vac. Sci. Technol. A* **38**, 022605 (2020).
- 25 Y. Gong, S. T. Misture, P. Gao, and N. P. Mellott, *J. Phys. Chem. C* **120**, 22358 (2016).
- 26 L. T. Zhuravlev, *Colloids Surf. A* **173**, 1 (2000).
- 27 J. A. Lercher, C. Gründling, and G. Eder-Mirth, *Catal. Today* **27**, 353 (1996).
- 28 G. A. Parks, *Chem. Rev.* **65**, 177 (1965).
- 29 H. Knözinger and P. Ratnasamy, *Catal. Rev.* **17**, 31 (1978).
- 30 J. E. Gozum and G. S. Girolami, *J. Am. Chem. Soc.* **113**, 3829 (1991).
- 31 M. D. Fryzuk, S. J. Rettig, A. Westerhaus, and H. D. Williams, *Inorg. Chem.* **24**, 4316 (1985).
- 32 G. A. Nesterov, V. A. Zakharov, V. V. Volkov, and K. G. Myakishev, *J. Mol. Catal.* **36**, 253 (1986).
- 33 X. Wang, Z. Guo, Y. Gao, and J. Wang, *J. Mater. Res.* **32**, 37 (2016).
- 34 Q. Xie, Y.-L. Jiang, C. Detavernier, D. Deduytsche, R. L. Van Meirhaeghe, G.-P. Ru, B.-Z. Li, and X.-P. Qu, *J. Appl. Phys.* **102**, 083521 (2007).
- 35 J. W. Elam, D. A. Baker, A. J. Hryn, A. B. F. Martinson, M. J. Pellin, and J. T. Hupp, *J. Vac. Sci. Technol. A* **26**, 244 (2008).